Colloid Polym Sci (2009) 287:225–230
DOI 10.1007/s00396-008-1971-2

ORIGINAL CONTRIBUTION

Comparative study on interaction of bovine serum albumin with dissymmetric and symmetric gemini surfactant by spectral method

Dan Wu · Guiying Xu · Yujun Feng · Yajing Wang · Yanyan Zhu

Received: 5 July 2008 / Revised: 8 October 2008 / Accepted: 18 November 2008 / Published online: 9 December 2008

Abstract The interaction between bovine serum albumin (BSA) with *N*, *N*′-bis(dimethylalkyl) ethylammonium dibromide ($C_{12}C_2C_m$, m=8, 12) was investigated by spectral methods. It can be seen that $C_{12}C_2C_8$ and $C_{12}C_2C_{12}$ mainly interact with tryptophan residues of BSA from synchronous fluorescence spectra. Fluorescence, far-UV, and near-UV circular dichrosim spectra of BSA are changed by addition of dissymmetric and symmetric gemini surfactant. For surfactant solution, the polarity of the microenvironment surrounding pyrene is lower while the fluorescence lifetime of it is longer and the microviscosity is higher in the presence of BSA than those in the absence of BSA. But compared with $C_{12}C_2C_{12}$, $C_{12}C_2C_8$ has lower binding ability with BSA due to the shorter hydrophobic tail and lower symmetry.

Keywords Bovine serum albumin (BSA) · *N*, *N*′-bis(dimethylalkyl)ethylammonium dibromide ($C_{12}C_2C_m$, m=8, 12) · Gemini surfactant · Interaction · Spectral method

D. Wu · G. Xu (✉) · Y. Wang · Y. Zhu
Key Laboratory of Colloid and Interface Chemistry,
Education Ministry, Shandong University,
Jinan 250100, People's Republic of China
e-mail: xuguiying@sdu.edu.cn

D. Wu
School of Chemistry and Chemical Engineering,
University of Jinan,
Jinan 250022, People's Republic of China

Y. Feng
Chengdu Institute of Organic Chemistry,
Chinese Academy of Sciences,
Chengdu 610041, People's Republic of China

Introduction

Protein–surfactant interaction has been of considerable research interest due to its application in drug delivery, cosmetics, and foods, and so on [1, 2]. It has been reported [3] that their interaction depends on protein and surfactant structures, as well as their concentrations. Once surfactant binds with protein, it may either stabilize or destabilize the conformation of protein and alter the function of protein. Therefore, it is important to understand the nature of protein–surfactant interaction.

Bovine serum albumin (BSA) is the protein commonly used for research purposes and as a reference in clinical analysis and biochemistry research because of its stability, water solubility and the wide capacity for binding bio-organic components. Its isoelectric point is 5.4 [4]. Up to now, the interaction between BSA and surfactants is mainly focus on the traditional surfactant such as CTAB, SDS, and Triton X-100 [5–12]. Less attention has been paid to BSA/gemini surfactant [13, 14], especially dissymmetric gemini surfactant. Gemini surfactant, a new class of amphiphilic molecules, is made up of two hydrophobic chains and two polar headgroups covalently attached by a spacer group [15–17]. Compared with single-chain surfactant, gemini surfactant has many unique properties such as higher surface activity, better solubility, and good foaming capability, etc. For dissymmetric gemini surfactant, it has more potential applications in synthesis of ordered porous materials than symmetric gemini surfactant owing to its unique properties [18]. So it is interesting to study the behaviors of BSA/dissymmetric gemini surfactant system.

Recently, we have investigated the interaction between symmetric gemini surfactant ($C_{12}C_2C_{12}$) and proteins [19, 20]. In continuation of our previous works, the interaction between dissymmetric gemini surfactant ($C_{12}C_2C_8$) and BSA

is studied by spectral methods including circular dichrosim (CD), synchronous, steady-state, and dynamic fluorescence. The results show that $C_{12}C_2C_8$ has lower binding ability with BSA because the hydrophobic tail of $C_{12}C_2C_{12}$ is longer than that of $C_{12}C_2C_8$. And the symmetry may be also an important factor for the interaction between gemini surfactant and protein.

Experimental

Materials

Bovine serum albumin was purchased from Sigma and was used as received without further purification. Cationic gemini surfactants, *N*, *N*′-bis (dimethylalkyl)ethylammonium dibromide ($C_{12}C_2C_m$, m=8, 12) were synthesized and characterized by ^{1}HNMR and elemental analysis [21]. The results are shown in Tables 1, 2, and 3. $C_{12}C_2C_{12}$ was synthesized by the quaternization of tetramethyl ethylenediamine and 1-bromododecane in isopropanol for 48 h. Then, the surfactant was recrystallized in acetone–ethanol mixtures for three times after evaporation of isopropanol. The white solid powder product ($C_{12}C_2C_{12}$) was obtained through vacuum drying for 24 h. $C_{12}C_2C_8$ was synthesized by using the following method: firstly, intermediate (C_2C_8) was synthesized by the quaternization of tetramethyl ethylenediamine and bromoalkane in acetone. The corresponding pure C_2C_8 was obtained in 60~70% yield after evaporation of isopropanol and recrystallization in ether for several times. Then, this compound and 1-bromododecane reacted in acetonitrile for 2~3 days. After evaporation, the residue was recrystallized for several times in acetone. Lastly, the white solid powder product ($C_{12}C_2C_8$) was obtained through vacuum drying 24 h. The purity of the gemini surfactants were examined using the ring method and almost no minimum was found in the surface tension curves (Fig. 1). The fluorescent probe, pyrene, was obtained from Sigma. The water used in the experiments was triply distilled by a quartz water purification system.

Circular dichrosim

The experiments were performed on a Jasco J-810 spectropolarimeter. In Far-UV condition (190~250 nm), a cell of 0.1 mm path length was used. In the near-UV region (250~320 nm), measurements were made in a cell of 10-mm path length. The α-helical, β-sheet, and the random coil contents were analyzed using the curve fitting method of the far-UV CD spectrum with the Jasco secondary structure manager.

Steady-state fluorescence

Fluorescence spectra and intensities were recorded on a Hitachi F-4500 Spectrofluorimeter. The fluorescence spectra of BSA were recorded with an excitation wavelength at 280 nm while pyrene spectra were recorded with fixed excitation wavelength at 335 nm.

Synchronous fluorescence spectra were acquired by the same spectrofluorometer. They were recorded, keeping the difference between excitation wavelength and emission wavelength fixed ($\Delta\lambda = \lambda_{em} - \lambda_{ex}$). When the $\Delta\lambda$ is at 20 or 60 nm, the synchronous fluorescence gives the characteristic information of tyrosine residues or tryptophan residues [22]. All the excitation and emission slits were set at 10/2.5 nm.

Fluorescence polarization was measured in the same spectrofluorometer using parallel and perpendicular polarizers. The steady-state polarization, *P*, obeys Eq. 1.

$$P = \frac{I_{\parallel} - I_{\perp}}{I_{\parallel} + I_{\perp}} \quad (1)$$

where $I_{\parallel}$ and $I_{\perp}$ are the fluorescence intensities in the parallel and vertical directions, respectively, to the incidence polarization, *P* is the observed polarization intensity of the probe.

Time-resolved fluorescence

Pyrene was used as fluorescence probe. The desired amount of pyrene was added to the surfactant solution directly and then the solution was stirred for 0.5 h. The concentration of pyrene was kept low to prevent excimer formation. All of the solutions were degassed by nitrogen for 5 min before the measurement to eliminate the influence of oxygen. Pyrene fluorescence decay curves were monitored by an FL-900 time-resolved fluorescence spectrophotometer from Edinburgh Analytical Instrument (excitation at 335 nm and emission at 385 nm). The excitation source was a hydrogen nanosecond flash lamp with a repetition rate of 40 kHz. For

Table 1 Elemental analysis results of the gemini surfactants

Sample	N/%		H/%		C/%	
	Measurement	Calculated	Measurement	Calculated	Measurement	Calculated
$C_{12}C_2C_8$	5.02	5.00	10.38	10.39	53.24	55.60
$C_{12}C_2C_{12}$	5.00	4.56	11.00	10.75	58.63	58.47

Table 2 ^{1}HNMR spectral data of intermediates

Groups in C_2C_8	CH_3	$(CH_2)_5$	N^+CCH_2	N^+ CH_2C	N $(CH_3)_2$	NCH_2CN^+	N^+CH_2CN	$N^+(CH_3)_2$
H number	3	10.2	2	2	5.7	2	2	5.7
δ	0.9	1.32	1.82	3.4	2.3	2.8	3.5	3.3
Groups in C_2C_{12}	CH_3	$(CH_2)_9$	N^+CCH_2	N^+ CH_2C	N $(CH_3)_2$	NCH_2CN^+	N^+CH_2CN	$N^+(CH_3)_2$
H number	3	18.4	2.1	2	6	2.1	2.1	6.1
δ	0.9	1.32	1.82	3.4	2.3	2.8	3.6	3.3

surfactant system, data were fit to single exponential. For surfactant–protein system, data were fit to biexponential decay. The goodness of the fit was determined by the χ^2 value ($\chi^2<1.1$) and examination of the residuals. For surfactant–protein system, the dominant contribution to the lifetime came from τ_1 and τ_2 was much less than τ_1. Therefore, the lifetime in surfactant–protein system was referred to τ_1 in the text.

All the experiments were performed at 25 °C.

Results and discussion

Far-UV CD spectra

In order to get the information about the secondary structure of proteins, the far-UV CD spectra for BSA are performed in the absence and presence of $C_{12}C_2C_8$, which is shown in Fig. 2. It can be seen that an α-helical structure of BSA is characterized by negative peaks at 208 and 218 nm. At low $C_{12}C_2C_8$ concentration ($\leq$0.1 mmol·L^{-1}), the CD spectra of $C_{12}C_2C_8$/BSA has no remarkable difference from that of BSA, suggesting that BSA maintains its natural secondary structure. However, at high $C_{12}C_2C_8$ concentration, the decrease in the negative ellipticity at 208 and 218 nm is observed. And the higher $C_{12}C_2C_8$ concentration, the less the α-helical content is. It is also found that addition of $C_{12}C_2C_8$ has a considerable effect on the percentage of β-sheet and random coil through calculation. Hence, it is deduced that $C_{12}C_2C_8$ at high concentration disrupts the secondary structure and leads to the unfolding of BSA.

Near-UV CD spectra

To study the structural alterations in more detail, the near-UV CD spectra, a useful probe for the tertiary structure of protein, are done in the absence and presence of $C_{12}C_2C_8$. As is shown in Fig. 3, the near-UV CD spectra of BSA between 250 nm and 320 nm have no remarkable change at low concentration (0.1 mmol·L^{-1}) of $C_{12}C_2C_8$. When the concentration of $C_{12}C_2C_8$ is above its critical micelle concentration (cmc) (2.0 mmol·L^{-1}), the near-UV CD spectra show significant changes. This implies that the binding of BSA with $C_{12}C_2C_8$ induces the changes of the microenvironment around aromatic amino acid residues and disulfide bonds [23].

Comparing with $C_{12}C_2C_{12}$ [19], $C_{12}C_2C_8$ has weaker effect on the far-UV and near-UV CD spectra. On the one hand, when surfactant concentration is 3.5 mmol·L^{-1}, the decrease of the α-helical content induced by $C_{12}C_2C_{12}$ is 14.1% while that induced by $C_{12}C_2C_8$ is 11.5% from the far-UV CD results, indicating $C_{12}C_2C_{12}$ causes BSA to an extended structure with exposed hydrophobic residues. On the other hand, when surfactant concentration is 2.0 mmol·L^{-1}, more obvious change is found in the near-UV CD spectra. Therefore, $C_{12}C_2C_{12}$ interacts with BSA more strongly than $C_{12}C_2C_8$ because it has longer hydrophobic tail and higher symmetry.

Microviscosity

Using the Eq. 2 developed by Shinitzky and Barenholz [24], the microviscosity (η) of different systems is calculated.

$$\eta = {}^{2P}/_{(0.46-P)} \tag{2}$$

It can be seen that the greater fluorescence polarization, the higher microviscosity is [25]. In this study, pyrene was used as a probe. The result shows that surfactant/BSA system provides a higher microviscosity than surfactant system without BSA, suggesting that pyrene motion is more restricted in the presence of BSA than in the absence of it.

Table 3 ^{1}HNMR spectral data of the gemini surfactants

Groups in $C_{12}C_2C_8$	CH_3	$(CH_2)_{14}$	$(N^+CCH_2)_2$	$(N^+CH_2C)_2$	$(NCH_3)_4$	$(N^+CH_2CN)_2$
H number	6.0	28.3	4.06	3.7	11.8	3.7
δ	0.9	1.2~1.5	1.82	3.7	3.3	4.2
Groups in $C_{12}C_2C_{12}$	CH_3	$(CH_2)_{18}$	$(N^+CCH_2)_2$	$(N^+CH_2C)_2$	$(NCH_3)_4$	$(N^+CH_2CN)_2$
H number	6	36	4	4	12	4
δ	0.9	1.2~1.5	1.82	3.54	3.34	4.52

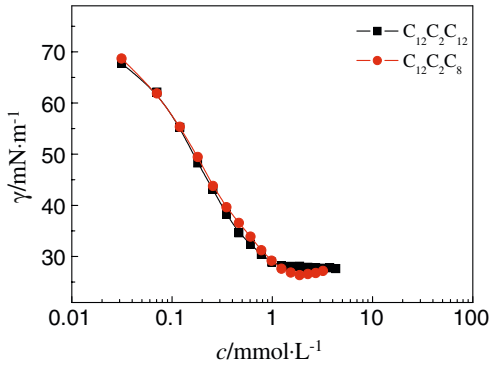

Fig. 1 Surface tension isotherms of different solutions

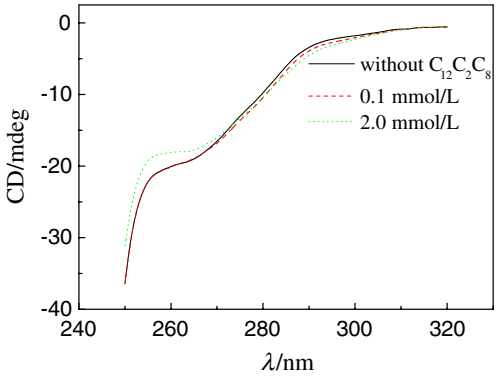

Fig. 3 Near-UV spectra of BSA at different concentration of $C_{12}C_2C_8$

But the microviscosities of $C_{12}C_2C_{12}$ and $C_{12}C_2C_{12}$/BSA are close to those of $C_{12}C_2C_8$ and $C_{12}C_2C_8$/BSA, respectively.

Micropolarity

The intensities ratio of the first and the third of the major vibrational peaks in pyrene's fluorescence spectrum (I_1/I_3), is sensitive to the microenvironmental polarity surrounding pyrene molecule [26–28]. The I_1/I_3 value decreases with increasing hydrophobicity. In order to study the effect of surfactant tail length, the change of I_1/I_3 value as a function of $C_{12}C_2C_{12}$ and $C_{12}C_2C_8$ concentration in the absence and presence of BSA is shown in Fig. 4. For surfactant solution, the curves show a sharp transition at its critical micelle concentration, which is around 0.9 mmol·L^{-1} for $C_{12}C_2C_{12}$ and 1.8 mmol·L^{-1} for $C_{12}C_2C_8$, suggesting that hydrophobic microdomains are formed. Comparing $C_{12}C_2C_{12}$ with $C_{12}C_2C_8$, the hydrophobicity increases as surfactant tail length increasing, leading to the decrease of the polarity of the microenvironment. From the I_1/I_3 value of surfactant at high concentration, it also can be seen that the molecular array in $C_{12}C_2C_{12}$ micelle is more compact than that in $C_{12}C_2C_8$ micelle.

However, addition of BSA induces a considerable decrease in the I_1/I_3 value at low surfactant concentration. The I_1/I_3 value at high concentration is close to that of pure surfactant. For 2 g·L^{-1} BSA solution, the I_1/I_3 value 1.27. For BSA/surfactant system, a very small decrease of the ratio occurs with surfactant concentration increasing, suggesting that pyrene migrates from the hydrophobic site on BSA to the micelle because the polarities of the microenvironments in BSA solution and the micelle are close. It also can be seen from Fig. 4 that the I_1/I_3 value in $C_{12}C_2C_8$/BSA system is higher than that in $C_{12}C_2C_{12}$/BSA system because hydrophobic effect between surfactant and BSA increases with surfactant tail length increasing.

The fluorescence lifetime of pyrene

Time-resolved fluorescence can give the information about microenvironmental changes, the dynamic behavior and the mean aggregation number of micelle [29–31]. The decay curves of pyrene fluorescence in 0.01 mmol·L^{-1} and 5 mmol·L^{-1} $C_{12}C_2C_8$ solutions are shown in Fig. 5. Obviously, the decay rate constant (k_0) in 5 mmol·L^{-1} $C_{12}C_2C_8$ solution is greater than that in 0.01 mmol·L^{-1} $C_{12}C_2C_8$ solution. As has been already pointed out [32, 33] that the fluorescence lifetime is equal to the reciprocal of the decay rate of the probe if there is no quencher, it is

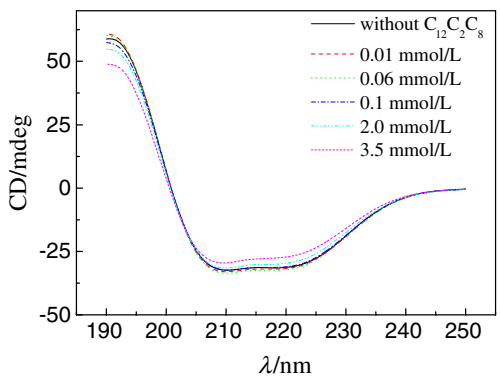

Fig. 2 Far-UV spectra of BSA at different concentration of $C_{12}C_2C_8$

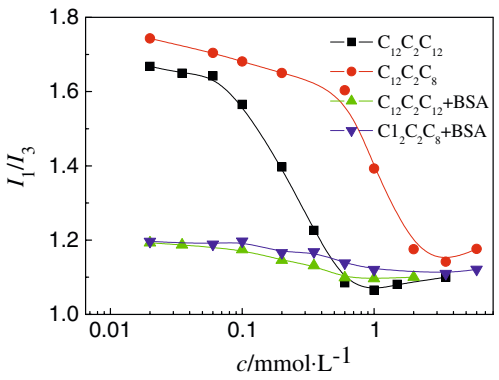

Fig. 4 Dependence of I_1/I_3 on surfactant concentration in different solutions

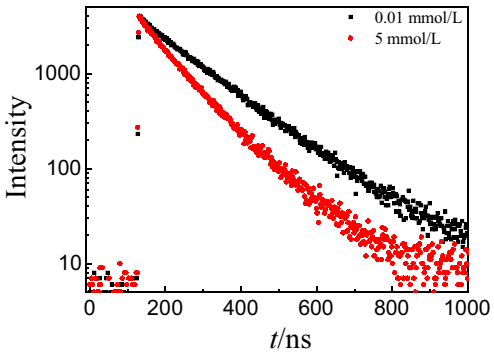

Fig. 5 Decay curves of pyrene fluorescence in $C_{12}C_2C_8$ solution

proposed that the lifetime is longer in 0.01 mmol·L^{-1} $C_{12}C_2C_8$ solution than that in 5 mmol·L^{-1} $C_{12}C_2C_8$ solution. Figure 6 shows pyrene fluorescence lifetime at different surfactant concentration. It can be seen that the lifetime of pyrene drops slightly with the concentration of $C_{12}C_2C_8$ increasing. Similar trend is also observed in CTAB system, but contrary trend is found in SDS and $C_{12}E_8$ systems [32]. Maybe the reason is that the bromide counterion, which quenches the pyrene fluorescence, is not replaced quantitatively from the micelle interface. So the fluorescence lifetime decreases.

However, in the presence of BSA, the lifetime becomes longer. Comparing $C_{12}C_2C_8$ system with BSA/$C_{12}C_2C_8$ system, it can be concluded that the weaker the polarity of the microenvironment, the longer the fluorescence lifetime of pyrene is. This law is in agreement with that in the literature [34, 35]. Comparatively small changes are observed when $C_{12}C_2C_8$ concentration is lower than 2.0 mmol·L^{-1}. Then the lifetime decreases to the value observed for the free $C_{12}C_2C_8$ micelle, suggesting that bromide counterions are also present near the interface of BSA-bound micelles at high $C_{12}C_2C_8$ concentration.

For $C_{12}C_2C_{12}$ and $C_{12}C_2C_{12}$/BSA systems, the dependences of the fluorescence lifetime of pyrene have the similar tendency on surfactant concentration with those of $C_{12}C_2C_8$ and $C_{12}C_2C_8$/BSA systems. The polarity of the microenvironment decreases as surfactant tail length increases, so the fluorescence lifetimes of pyrene in $C_{12}C_2C_{12}$ and $C_{12}C_2C_{12}$/BSA systems are longer than those in $C_{12}C_2C_8$ and $C_{12}C_2C_8$/BSA systems, respectively.

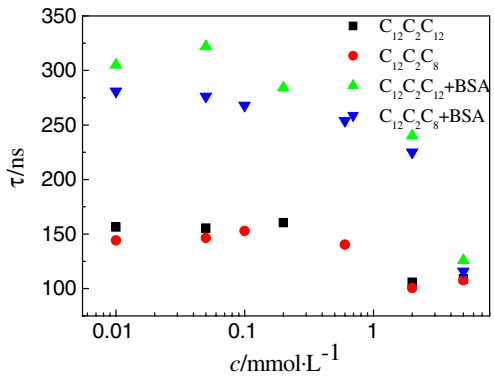

Fig. 6 Pyrene fluorescence lifetime versus surfactant concentration

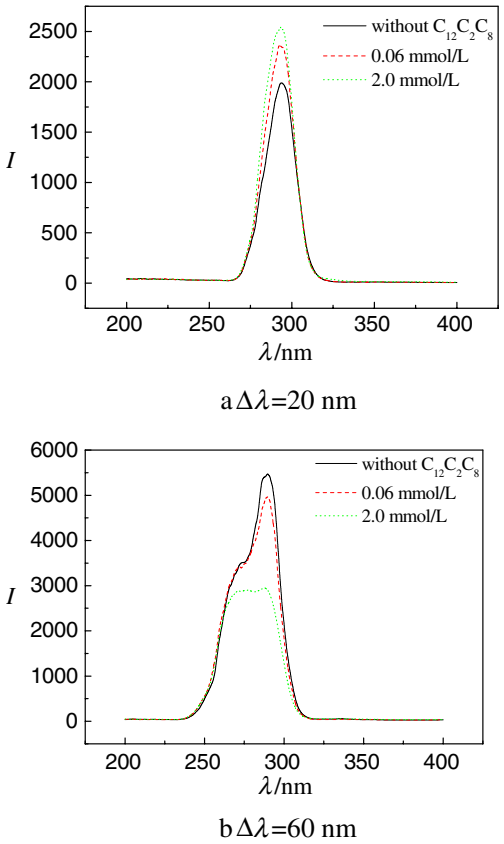

Fig. 7 Synchronous spectra of BSA at different concentration of $C_{12}C_2C_8$

Synchronous spectra

Synchronous fluorescence spectra of BSA are shown in Fig. 7. The fluorescence intensity of BSA for $\Delta\lambda$ =60 nm is higher than that for $\Delta\lambda$ =20 nm, indicating that the fluorescence peak at 341 nm should be mainly contributed

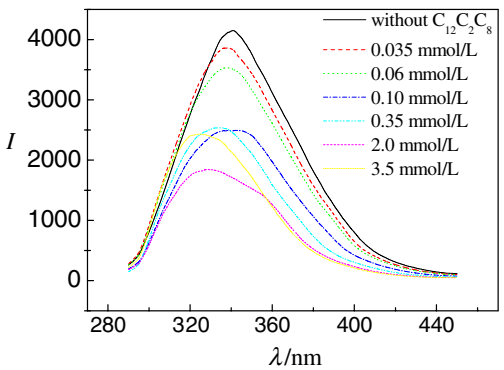

Fig. 8 Fluorescence spectra of BSA at different $C_{12}C_2C_8$ concentration

by tryptophan. On the other hand, the fluorescence intensity of BSA decreases for $\Delta\lambda$ =60 nm and increases for $\Delta\lambda$ = 20 nm when $C_{12}C_2C_8$ is added. However, the decrease of the fluorescence intensity for $\Delta\lambda$ =60 nm is much larger than the increase for $\Delta\lambda$ =20 nm at the same concentration of $C_{12}C_2C_8$. Therefore, $C_{12}C_2C_8$ mainly interacts with tryptophan residues [25] and this conclusion is also found in $C_{12}C_2C_{12}$/BSA system.

Fluorescence spectra

Fluorescence spectra of BSA at different $C_{12}C_2C_8$ concentration are shown in Fig. 8. When $C_{12}C_2C_8$ is added to BSA solution, the fluorescence intensity decreases and a blue shift from 341 nm to 327 nm is observed in the maximum emission peak, suggesting that trp residues are exposed to a more hydrophobic environment. This phenomenon is ascribed to the formation of BSA/$C_{12}C_2C_8$ complex. Then, the fluorescence intensity increases gradually when $C_{12}C_2C_8$ concentration is above its cmc (>2.0 mmol·L^{-1}), which is due to partially denatured BSA. It is reported that similar trend is also found in single-chain surfactant/BSA such as CTAC/BSA and HPS-BSA [36] and double-chains surfactant/BSA such as $C_{12}C_2C_{12}$/BSA [19]. According to the literature [13], the change of fluorescence spectra implies that BSA conformation changes with $C_{12}C_2C_8$ concentration increasing, which is also verified by the CD spectra.

Conclusion

$C_{12}C_2C_8$/BSA system provides a higher microviscosity than $C_{12}C_2C_8$ system and the microviscosity increases with $C_{12}C_2C_8$ concentration increasing. At low surfactant concentration, the fluorescence lifetime of pyrene in BSA/$C_{12}C_2C_8$ complexes is higher than that in $C_{12}C_2C_8$ system while the polarity of the microenvironment has contrary phenomenon and at high surfactant concentration, the lifetime of pyrene and the micropolarity reach the values corresponding to free micelles. At the same time, the conformational changes in BSA are monitored by fluorescence and CD spectra. From those results, it can be deduced that $C_{12}C_2C_8$ can interact with BSA via the electrostatic forces and hydrophobic forces, but has weaker binding ability with BSA than $C_{12}C_2C_{12}$. So spectroscopy is a good and important method to study the interaction between protein and surfactant.

Acknowledgment The authors are grateful for the financial support from the Natural Science Foundation of Shandong Province (Y2004B06) and Key Laboratory of Colloid and Interface Chemistry (Shandong University), Ministry of Education (200713).

References

1. Goddard ED, Ananthapadmanabhan KP (1993) Interaction of surfactants with polymers and proteins. CRC, New York
2. Miller R, Fainerman VB, Makievski AV, Krägel J, Grigoriev DO, Kazakov VN, Sinyachenko OV (2000) Adv Colloid Interface Sci 86:39
3. Antipova AS, Semenova MG, Belyakova LE, Il'in MM (2001) Colloid Surf B 21:217
4. Shi Q, Zhou Y, Sun Y (2005) Biotechnol Prog 21:516
5. Sukow WW, Sandberg HE, Lewis EA, Eatough DJ, Hansen LD (1980) Biochemistry 19:912
6. Díaz X, Abuin E, Lissi E (2003) J Photochem Photobiol A 155:157
7. Grigoriev DO, Derkatch S, Krägel J, Miller R (2007) Food Hydrocoll 21:823
8. Gelamo EL, Itri R, Alonso A, Silva JVD, Tabak M (2004) J Colloid Interface Sci 277:471
9. Tribout M, Paredes S, González-Mañas JM, Goñi FM (1991) J Biochem Biophys Methods 22:129
10. Ding YH, Shu Y, Ge LL, Guo R (2007) Colloid Surf A 298:163
11. Valstar A, Almgren M, Brown W (2000) Langmuir 16:922
12. Turro NJ, Lei XG, Ananthapadmanabhan KP, Aronson M (1995) Langmuir l1:2525
13. Pi YY, Shang YZ, Peng CJ, Liu HL, Hu Y, Jiang JW (2006) Biopolymers 83:243
14. Li YJ, Wang XY, Wang YL (2006) J Phys Chem B 110:8499
15. Menger FM, Keiper JS (2000) Angew Chem Int Ed 39:1906
16. Zana R (2002) Adv Colloid Interface Sci 97:205
17. Rosen MJ (2004) Surfactants and interfacial phenomena, 3rd edn. Wiley, New York
18. Romero FJ, Jiménez C, Huc I, Oda R (2004) Microporous Mesoporous Mater 69:43
19. Wu D, Xu GY, Sun YH, Zhang HX, Mao HZ, Feng YJ (2007) Biomacromolecule 8:708
20. Wu D, Xu GY, Feng YJ, Li YM (2007) Int J Biol Macromol 40:345
21. Sun YH, Dong HW, Feng YJ, Chen Z (2006) Acta Chimi Sin 64:1925
22. Wang F, Yang JH, Wu X, Sun CX, Liu SF, Guo CY, Jia Z (2005) Chem Phys Lett 409:14
23. De S, Girigoswami A, Das S (2005) J Colloid Interface Sci 285:562
24. Shinitzky M, Barenholz Y (1978) Biochim Biophys Acta 515:367
25. Wang F, Yang JH, Wu X, Wang XB, Sun CX, Liu SF, Guo CY (2006) Biochimie 88:121
26. Wang X, Li Y, Wang J, Wang Y, Ye J, Yan H, Zhang J, Thomas RK (2005) J Phys Chem B 109:12850
27. Mylonas Y, Karayanni K, Staikos G, Koussathana M, Lianos P (1998) Langmuir 14:6320
28. Panmai S, Prud'homme RK, Peiffer DG, Jockusch S, Turro NJ (2002) Langmuir 18:3860
29. Guan JQ, Tung CH (1998) J. Colloid Interface Sci 208:90
30. Yin HQ, Lei S, Zhu SB, Huang JB, Ye JP (2006) Chem Eur J 12:2825
31. Feitosa E, Brown W, Wang K, Barreleiro PCA (2002) Macromolecules 35:201
32. Vasilescu M, Angellescu D, Almgren M, Valstar A (1999) Langmuir 15:2635
33. Deo N, Jockusch S, Turro NJ, Somasundaran P (2003) Langmuir 19:5083
34. Shen Q, Li GZ, Huang YZ, Ye JP (1999) Acta Physico-Chimica Sinica 15:216
35. Dai YH, Wu FP, Li MZ, Wang EJ (2004) Acta Chim Sin 62:823
36. Gelamo EL, Tabak M (2000) Spectrochim Acta A 56:2255